



## Mathematical modelling and simulation of an adjustable-stiffness spring

J.M. Chacón <sup>(a)</sup>, A. González Rodríguez <sup>(b)</sup>, A. Donoso <sup>(c)</sup>, A.G. González Rodríguez <sup>(d)</sup>

- <sup>(a)</sup> ETSII, Institute of Applied Mathematics in Science and Engineering, Universidad de Castilla-La Mancha, Spain.  
<sup>(b)</sup> ETSII, Department of Applied Mechanics, Universidad de Castilla-La Mancha, Spain.  
<sup>(c)</sup> ETSII, Department of Mathematics, Universidad de Castilla-La Mancha, Spain.  
<sup>(d)</sup> ETSII, Department of Electronic Engineering and Automation, Universidad de Jaén, Spain.

### Article Information

#### Keywords:

Compliant-actuators  
Adjustable-stiffness  
Large displacements  
Leaf spring.

#### Corresponding author:

J.M. Chacón  
Tel.: +34 926 29 53 00  
Fax.: +34 926 29 53 61  
e-mail: [jesusmiquel.chacon@uclm.es](mailto:jesusmiquel.chacon@uclm.es)  
Address: Edificio Politécnico s/n  
13171, Ciudad Real, Spain.

### Abstract

An adjustable-stiffness actuator composed of two antagonistic non-linear springs is proposed in this paper. The elastic device consists of two pairs of leaf springs working in pure bending under large displacement hypothesis. Owing to this geometric non-linearity, the global stiffness of the actuator can be adjusted by modifying the shape of the leaf springs. A mathematical model has been developed in order to predict the mechanical behaviour of our proposal. The non-linear differential equation derived from the model is solved, obtaining large stiffness variations.

### 1 Introduction

In most of the industrial activities where robots have been introduced, a stiff performance is preferred to fulfill the metrics based on movement accuracy, load capacity and easy trajectory tracking control. In industrial activities, reducing the stiffness protects the robot against possible impacts with human operators or other elements when working in unstructured environments, and facilitates dexterous tasks such as polishing or peg-in-hole. However, compliance deteriorates the robot accuracy and load capacity, and makes the control more difficult. A robot able to adapt its compliance/stiffness according to the type of task or movement could maintain the advantages of both stiff manipulators and safe-dexterous compliant ones [1]. In line with this application, variable stiffness/compliance actuators have also been successfully included in compliant endoscopes, robotic surgery, prosthetics and robots aiding in rehabilitation therapy.

Very different in nature are the applications in which the natural frequency is changed. This is the case of some adaptive vibration absorbers in which the stiffness is adjusted according to the varying excitation frequency [2, 3, 4, 5]. These adaptive absorbers have been attached to buildings, floating rafts, automobiles and, in general, rotating machines where excessive vibrations produce fatigue, discomfort, increased maintenance and deteriorated performance. Also interesting is the case of efficient legged robots based on the concept of passive dynamic walking [6, 7, 8], in which adaptable compliance actuators allows the robot to change its natural walking speed.

Recent research dealing with variable stiffness actuators has predominantly focused on four principal technologies: electroactive polymers (EAPs), pneumatic actuators, electrical motors with active compliance and adjustable-stiffness elastic elements.

EAPs are polymers whose shape is modified when they are supplied a voltage [9]. They are able to undergo a large amount of deformation, which makes them the suitable option in guide wires, leads and catheters. Its main drawback is its high non-linearity.

Pneumatic artificial muscles are typically contractile devices operated by pressurized air, which can be varied to regulate the muscle stiffness. They require an antagonist setup to generate a restoring movement or force. The majority of the pneumatic systems are based on the McKibben muscle [10] which bulges, shortens and generates a contraction force when it is inflated. The main drawbacks are low efficiency, lack of precision and that they need an air compressor.

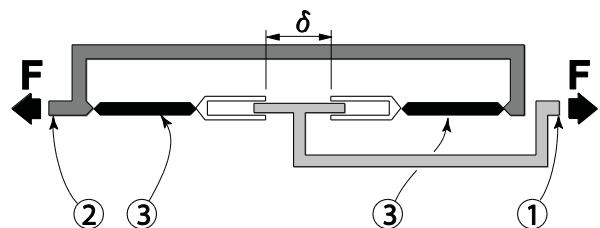


Fig. 1 Adjustable-stiffness spring composed by two antagonistic non-linear springs.

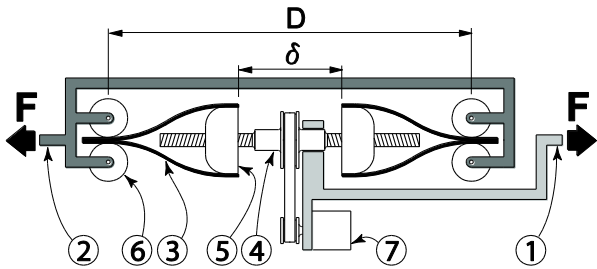


Figure 2: Proposal of an adjustable-stiffness spring using leaf springs for large displacements.

Force control based on electrical motors with active compliance is the technique used by most of compliant industrial robots. It does not include a real elastic element. Instead, a force sensor measures the external force/torque applied to the end-effector when interacting with the environment and adjusts the forces applied to the joints in order to imitate and tune a spring. This method permits a compliant operation without losing accuracy or load capacity. Its main disadvantage is that it requires a force sensor and that it drains a constant energy even when no work is being performed. The impedance control [11] is the most implemented method. Some of its limitations can be reduced by introducing a constant stiffness coupling attached to the end-effector, like in the series elastic actuator [12].

Adjustable-stiffness elastic elements are based on an elastic passive element whose stiffness can be adjusted. These techniques introduce the possibility of regulating the natural frequency of the element where the joint is included. Three concepts can be differentiated ([8]):

- The variable stiffness actuators based on an antagonistic setup consisted of two non-linear springs working simultaneously and in opposition. An example of this technique is the design proposed in [13] using rolamites with quadratic characteristics. The quadratic characteristic decouples joint stiffness and deflection, and it has also been pursued in [14, 15]. Other models based on an antagonistic setup are the ones presented in [16, 17] or the ones using pneumatic artificial muscles.
- The Structure-Controlled Stiffness concept is based on the variation of the effective length of a compliant element. Examples of this group is the Jack Spring [18] or the ones presented in [19, 20]. The design from Gonzalez et al. [21] falls on this structure, giving high stiffness variation.
- In the Mechanically-Controlled Stiffness actuators, the adaptable compliance is accomplished by an electrical motor that modifies the force exerted by an elastic element [8]. A controlled non-linear relationship between force/torque and displacement/rotation permits the adjustment of the effective stiffness.

This paper presents an adjustable-stiffness spring based on a compound leaf spring made of strips of sheet metal clamped at each end. The scheme is similar to the vibration absorber of [2], although this new actuator does not require additional masses and the movement is directed in the longitudinal direction instead of the transversal one. This feature leads to a different method to vary the stiffness.

The layout of the paper is organized as follows. Section 2 explains the set-up of the proposed solution and the way it works. Section 3 includes the mathematical model and the results obtained from its formulation. Section 4 shows the principal aspects related to the fabrication of the prototype. Finally, the conclusions derived during the development of the scheme are presented in Section 5.

## 2 An adjustable-stiffness spring

The stiffness of a spring is the relationship between a force applied to both extremes of the spring and the displacement that it experiments. As previously mentioned, an antagonistic set-up is one of the possibilities to build an adjustable stiffness spring. Fig. 1 shows a scheme that can vary its stiffness according to this concept. The elastic elements are labeled as 3 and bars where are located forces are labeled as 1 and 2. By modifying the distance  $\delta$ , the springs are pre-compressed, and consequently the global stiffness of the device is changed. However, this variation will occur only if the springs have a non-linear function between force and displacement. Non-linear springs can be built by means of helicoidal springs with a non-constant step between spires. In [13] an adjustable-stiffness spring is proposed using two rolamite springs with a quadratic function between force and displacement.

Following the scheme of fig. 1, this paper proposes an adjustable-stiffness spring with antagonistic springs, working in pure bending under large displacements, as it is shown in fig. 2. Such springs have important advantages: they can work with very high forces (higher than rolamite springs, rubber bands, polymer, etc) and they can change their stiffness in a highly wide range of values. We can obtain stiffness variations of 1500%, much higher than using helicoidal springs, magnetoelastic materials or rolamite springs.

The description of the mechanism is as follows. Bars where force is applied are labeled as 1 and 2 in fig. 2. Four leaf springs working in pure bending under large displacements are labeled as 3. Label 4 refers to a screw attached to bar 1 through a rotational joint. Turning the screw forces the displacement of the semi-cylinder shaped nut (label 5), to which the leaf springs are clamped. This action modifies the distance  $\delta$  between semi-cylinders, changing the shape of the leaf springs, and consequently the global stiffness as well. An electric motor, labeled as 7, moves the screw through a pulley. The screw has right-handed thread for right side and left-handed thread for left side, and therefore distance  $\delta$  is symmetrically changed. In consequence the spring varies its stiffness without changing its equilibrium position in absence of forces.

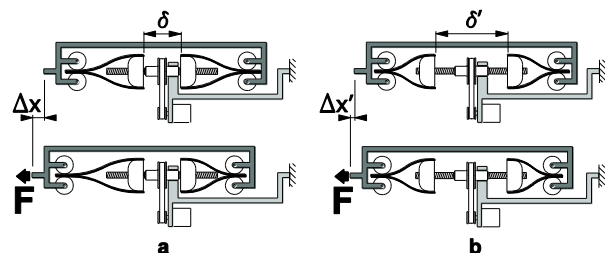


Figure 3: Different positions of the compliant-actuator on varying  $\delta$ ; (a) low stiffness, (b) high stiffness configuration.

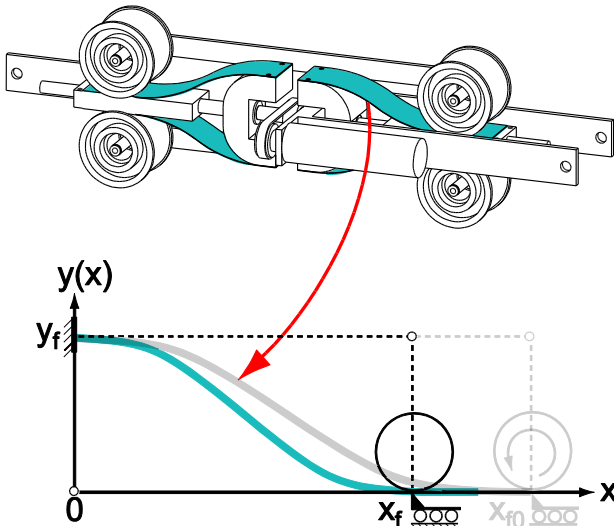


Figure 4: A 3D-CAD model of the prototype (above) and a structural model of one of the leaf springs (below).

Leaf springs must be protected from excessive curvatures. Hence, a protection system has been included which is composed of four rollers (label 6) and two semi-cylinders (label 5) where the leaf springs are clamped. Accordingly, the protection system ensures that leaf springs do not plasticize when they adopt their maximum curvature. Fig. 3 shows different positions of the spring by modifying distance  $\delta$ . Fig. 3(a) and 3(b) show a low and high stiffness configuration, respectively. If  $\delta < \delta'$ , the displacement of the spring will be  $\Delta x > \Delta x'$ , for the same force  $F$ .

### 3 Mathematical modelling

In this section a mathematical model of the aforementioned elastic device is developed. Fig. 4 shows a 3D-CAD model of the prototype. As commented before, the global stiffness of the actuator is adjusted by modifying the shape of the leaf springs. Notice that no longitudinal compressive force is applied to the leaf springs by the rollers (label 6), meaning that buckling is not considered in this case. Having this in mind, each one of the leaf springs can be modeled like a beam-type structure clamped in its inner extreme and with horizontal displacement-free in its outer extreme, working in bending only, but under large displacement hypothesis. That is the reason why the curvature expression cannot be linearized as usual. Hence the deformed shape is given by the one that minimizes the elastic potential energy, that is,

$$U(Y) = \frac{1}{2} EI \int_0^L \frac{Y''(s)^2}{1 - Y'(s)^2} ds$$

where  $Y(s)$  is the deformed shape as a function of  $s$ , the curvilinear coordinate, measured along the arc length described by the leaf spring. The term  $EI$ , known as the flexural stiffness, is the product of the Young's modulus,  $E$ , and  $I$ , the moment of inertia of the cross-sectional area of the leaf spring with respect to the bending axis, and  $L$  is the length of the leaf spring, which can be changed by modifying the rollers position.

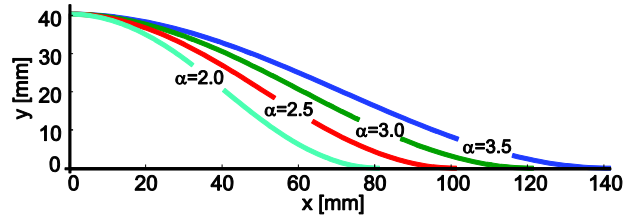


Figure 5: Shape of the leaf spring for different aspect ratio values.

As the energy functional  $U$  is strictly convex in the pair  $(Y, Y')$ , we can state that  $Y(s)$  is the unique solution of its associated Euler-Lagrange equation [22]

$$\frac{d}{ds} \left( \frac{d}{ds} \left( EI \frac{Y''(s)}{(1 - Y'(s)^2)^{1/2}} \right) \frac{1}{(1 - Y'(s)^2)^{1/2}} \right) = 0,$$

where  $s \in (0, L)$ , with  $L$  unknown. By using the change of variables

$$s(x) = \int_0^x \sqrt{1 + y'(t)^2} dt, \quad \text{with} \quad y(x) = Y(s),$$

we arrive at this (apparently) more treatable differential equation in Cartesian coordinates

$$\frac{d^2}{dx^2} \left( EI \frac{y''(x)}{(1 - y'(x)^2)^{3/2}} \right) = 0, \quad 0 < x < x_f,$$

where now  $x_f$  is the (known) horizontal distance between the extremes of the leaf spring, with the boundary conditions (see Figure 4)

$$y(0) = y_f, \quad y'(0) = y(x_f) = y'(x_f) = 0,$$

meaning that the leaf spring is clamped in the upper extreme, that is,  $y_0(0) = 0$ , and the contact point with the roller can be modeled as a pinned condition with no rotation, that is,  $y'(x_f) = 0$ . Even though this new differential equation is highly non-linear, for this particular case and after having integrated twice, it is possible to reduce it to one with separate variables (using a new change of variables,  $w(x) = y_0(x)$ , for instance), and therefore to find the solution in close form,

$$y(x) = y_f + \int_0^x \frac{a(t^2 - x_f t)}{\sqrt{1 - a^2(t^2 - x_f t)^2}} dt, \quad 0 \leq x \leq x_f,$$

where the parameter  $a$  is obtained by imposing that  $y(x_f) = 0$ , that is,  $a$  is numerically computed from the integral equation

$$y_f + \int_0^{x_f} \frac{a(t^2 - x_f t)}{\sqrt{1 - a^2(t^2 - x_f t)^2}} dt = 0.$$

Fig. 5 shows the shapes obtained for different values of the aspect ratio,  $\alpha = x_f/y_f$ . Once the deformed shapes have been obtained, it is easy to compute the stored energy (in one leaf spring) as a function of  $\alpha$  (see fig. 6).

Assume a spring displacement  $d = x_{f0} - x_f$ , where  $x_{f0}$  is the horizontal distance between the extremes of the leaf spring for an initial configuration (see fig. 4). Computing both the first derivative and the second derivative of the energy (for all of the four leaf springs working together) with respect to the displacement  $d$ , we obtain the theoretical family of curves for both force-displacement and stiffness-displacement (see fig. 7 and 8, respectively).

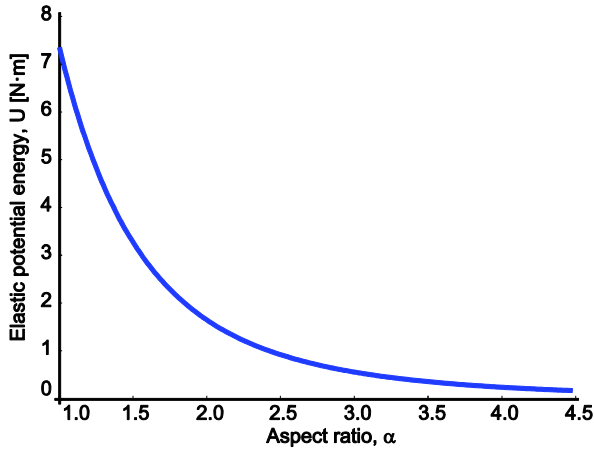


Figure 6: Elastic potential energy of a leaf spring versus aspect ratio.

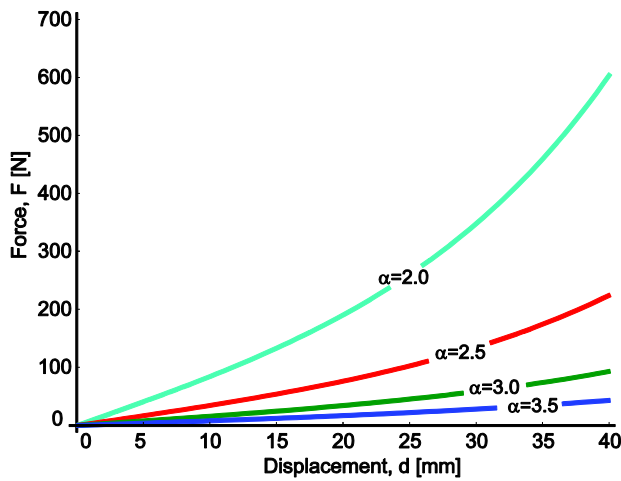


Figure 7: Force-displacement curves for different aspect ratio values.

#### 4 Fabrication of the prototype

This section is devoted to describe some aspects concerning the design process and fabrication of the prototype. It is important to notice that before testing the prototype, the deformed shape of one leaf spring was measured by means of a tridimensional coordinate measuring machine, showing a similar profile that the one obtained from the mathematical model.

The first step in the design process of the prototype consists in defining the dimensions of each one of the leaf springs. In this case, we have chosen a leaf spring with a width  $w = 50 \times 10^{-3}$  m and a thickness  $t = 0.5 \times 10^{-3}$  m. Its length is determined by the aspect ratio  $\alpha$  of the spring. More specifically, the prototype has a variable aspect ratio between  $\alpha_0 = 3.5$  and  $\alpha_1 = 2.0$ . Once the geometric parameters of the prototype have been fixed, both the roller radius and the semi-cylinder radius that ensure no yielding of the leaf spring are computed. The classic formula for determining the bending stress in a bar under simple bending is:

$$\sigma = \frac{M}{I} y_{max} \tag{1}$$

where  $\sigma$  is the bending stress,  $M$  is the moment about the neutral axis and  $y_{max}$  is the perpendicular distance to

the neutral axis (in this case  $y_{max} = t/2$ ). On the other hand, the ratio between the bending moment  $M$  and the radius of curvature  $R$  can be written as:

$$M = \frac{EI}{R} \tag{2}$$

Replacing equation (2) in (1), we obtain the expression of the limit radius of the bar in elastic region as:

$$R = \frac{Et}{2\sigma_y} \tag{3}$$

where  $\sigma_y$  is the yield stress. From (3), and using the following values:  $E = 2.1 \times 10^{11}$  N/m<sup>2</sup>,  $t = 0.5 \times 10^{-3}$  m,  $\sigma_y = 1500$  MPa, the radius of the protection system (label 5 and 6) is given by  $R = 35 \times 10^{-3}$  m.

As the mathematical model does not take into account the friction, we have tried to reduce it between mechanical elements of the prototype as much as possible, in order to experimentally obtain the range of stiffness expected from the theoretical model. In this way, the rollers (label 6) have been made of polyamide material, which exhibits a low coefficient friction. In addition, each axis roller is supported by two single-row deep groove ball bearings. Another important aspect in the design process has been the accuracy in changing the distance  $\delta$  between semi-cylinders (label 5), which defines the aspect ratio  $\alpha$  of the leaf spring, that is,

$$\alpha = \frac{D - \delta}{2y_f} \tag{4}$$

where  $D$  is the horizontal distance between the centers of the rollers (see fig. 2), and has been given a value of  $345 \times 10^{-3}$  m, and  $y_f = 40.5 \times 10^{-3}$  m. With this aim, a double-row angular contact ball bearing has been attached to the screw (label 4). Furthermore, in order to reduce the friction with the screw, each semi-cylinder has a bronze bearing. Fig. 9 shows the manufactured prototype.

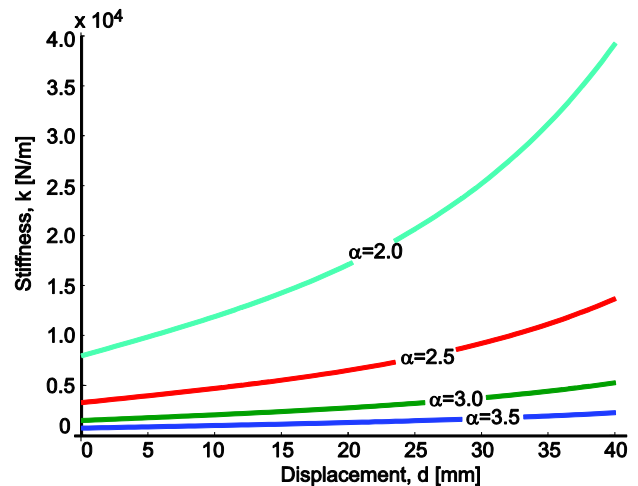


Figure 8: Stiffness-displacement curves for different aspect ratio values.

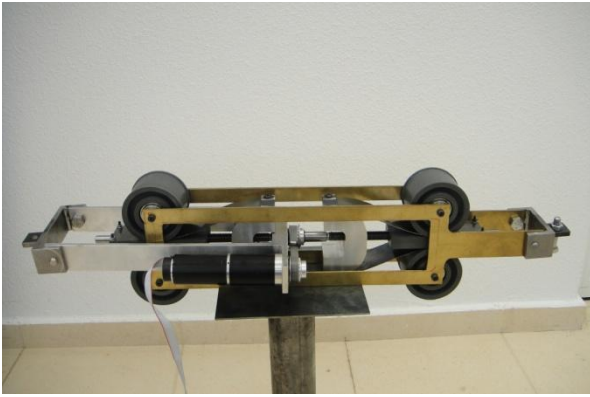


Figure 9: Prototype of adjustable-stiffness spring.

## 5 Conclusion

The present paper proposes a new model of an adjustable-stiffness spring. The proposed device has four leaf springs with non-linear elastic deformations. The geometry of the leaf spring can be modified by means of an electric motor that adjusts the stiffness of the spring to the desired value. The most important characteristic is its large stiffness range (with variations greater than 1500%), and its scalability for working with very high and very low loads. These characteristics allow the spring to be used for different purposes, like robotics, or vibration cancelation. All of these applications need different values of the stiffness and of its range of variation. This paper also proposes an analytical model that allows the leaf springs to be dimensioned for every specific purpose. Finally, a prototype of the spring has been built. In future works the prototype will be test in order to verify the behavior of the system and the accuracy of the analytical model.

## Acknowledgement

This work is supported by the Spanish Ministerio de Educación y Ciencia MTM2010-19739, Spanish Ministerio de Ciencia e Innovación DPI2009-10078, co-financed by the European Regional Development Fund, and Junta de Comunidades de Castilla - La Mancha PAI08-0286-4871 and PCI-08-0084 (Spain).

## References

- [1] S. Sugano, S. Tsuto, I. Kato. *Force control of the robot finger joint equipped with mechanical compliance adjuster*. Proceedings of IEEE/RSJ, International Conference on Intelligent Robots and Systems, 1992, Raleigh (USA), 3, pp. 2005-2013.
- [2] P.L. Walsh, J.S. Lamancusa. *A variable stiffness vibration absorber for minimization of transient vibrations*. Journal of Sound and Vibration, 158, 2 (1992) pp. 195-211.
- [3] H.L. Sun, K. Zhang, P.Q. Zhang, H.B. Chen. *Application of dynamic vibration absorbers in floating raft system*. Applied Acoustics, 71, 3 (2010) pp. 250-257.
- [4] K. Yamamoto, T. Yamamoto, H. Ohmori, A. Sano. *Adaptive feedforward control algorithms for active vibration control of tall structures*. Proceedings of IEEE, International Conference on Control Applications, 1997, Grenoble (France), pp. 736-742.
- [5] M.J. Brennan. *Some recent developments in adaptive tuned vibration absorbers/neutralisers*. Shock and Vibration, 13, 4-5 (2006) pp. 531-543.
- [6] T. McGeer. *Passive dynamic walking*. International Journal of Robotics Research, 9, 2 (1990) pp. 62- 82.
- [7] S. Collins, A. Ruina, R. Tedrake, M. Wisse. *Efficient bipedal robots based on passive-dynamic walkers*. Science, 307, 5712 (2005) pp. 1082-1085.
- [8] R. Van Ham, B. Vanderborght, M. Van Damme, B. Verrelst, D. Lefeber. *MACCEPA: the mechanically adjustable compliance and controllable equilibrium position actuator for controlled passive walking*. Proceedings of IEEE/ICRA, International Conference on Robotics and Automation, 2006, Orlando (USA), pp. 2195-2200.
- [9] EAP Material and Product Manufactures. Website: <http://ndeaa.jpl.nasa.gov/nasande/lommas/eap/EAP-material-products.htm>, 2008.
- [10] H.F. Schulte. *The characteristics of the McKibben artificial muscle*. In Application of external power in prosthetics and Orthotics, publication 874, National Academy of Science National Research Council, Washington DC, 1961, pp. 94-115.
- [11] N. Hogan. *Impedance Control: An Approach to Manipulation*. Proceedings of American Control Conference, 1984, San Diego (USA), pp. 304- 313.
- [12] G.A. Pratt, M.M. Williamson. *Series elastic actuators*. Proceedings of IEEE/RSJ, 1995, Pittsburgh (USA), 1, pp. 399- 406.
- [13] C. English, D. Russell. *Implementation of variable joint stiffness through antagonistic actuation using rolamite*. Mechanism and Machine Theory, 34, 1 (1999) pp. 27-40.
- [14] S.A. Migliore, E.A. Brown, S.P. DeWeerth. *Biologically Inspired Joint Stiffness Control*. Proceedings of IEEE/ICRA, International Conference on Robotics and Automation, 2005, Barcelona (Spain), pp. 4508- 4513.
- [15] K. Koganezawa, T. Inaba, T. Nakazawa. *Stiffness and Angle Control of Antagonistically driven joint*. Proceedings of Biomedical Robotics and Biomechatronics, BioRob, 2006, Pisa (Italy), pp. 1007-1013.
- [16] A. Bicchi, G. Tonietti. *Fast and soft arm tactics: Dealing with the safety-performance trade-off in robot arms design and control*. IEEE Robotics Automation Magazine, 11, 2 (2004) pp. 2233.
- [17] J.W. Hurst, J. E. Chestnutt, A.A. Rizzi. *The actuator with mechanically adjustable series compliance*. IEEE Transactions on Robotics, 26, 4 (2010) pp. 597-606.
- [18] K. Hollander, T. Sugar. *Concepts for compliant actuation in wearable robotic systems*. Proceedings of US-Korea Conference Science, Technology and Entrepreneurship, 2004, North Carolina.
- [19] T. Morita, S. Sugano. *Design and development of a new robot joint using a mechanical impedance adjuster*. Proceedings of IEEE/ICRA, International Conference on Robotics and Automation, 1995, Nagoya (Japan), 3, pp. 2469-2475.
- [20] T. Morita, S. Sugano. *Development of an anthropomorphic force-controlled manipulator WAM-10*. Proceedings of the 8th International Conference on Advanced Robotics, ICAR, 1997, Monterey (USA), pp. 701-706.
- [21] A. González Rodríguez, N. Nava-Rodríguez, A. G. González Rodríguez. *Design and validation of a novel actuator with adaptable compliance for application in human-like robotics*. Industrial Robot: An International Journal, 36, 1 (2009) pp. 84-90.
- [22] Troutman, J. L. *Variational Calculus and Optimal Control*, Springer-Verlag, 1996.